Available online at www.sciencedirect.com
ScienceDirect
Trans. Nonferrous Met. Soc. China 24(2014) 368−372
Transactions of Nonferrous Metals Society of China
www.tnmsc.cn

Texture of friction stir welded Ti−6Al−4V alloy

Li ZHOU[1,2,3], Hui-jie LIU[1], Lin-zhi WU[3]

1. State Key Laboratory of Advanced Welding and Joining, Harbin Institute of Technology, Harbin 150001, China;
2. Shandong Provincial Key Laboratory of Special Welding Technology, Harbin Institute of Technology at Weihai, Weihai 264209, China;
3. Center for Composite Materials and Structures, Harbin Institute of Technology, Harbin 150001, China

Received 7 February 2013; accepted 7 May 2013

Abstract: The $\alpha+\beta$ titanium alloy, Ti−6Al−4V, was welded by friction stir welding using a W−Re pin tool, and the defect-free weld was produced with proper welding parameters. Texture of the Ti−6Al−4V friction stir weld was studied by orientation imaging microscopy. The as-received Ti−6Al−4V sheet mill annealed was composed of elongated primary α and transformed β. A typical rolling texture was observed in the base material. The microstructure of the stir zone was significantly different from that of the base material. The stir zone was characterized by the presence of considerable amount of equiaxed dynamically recrystallized grains and a texture around $\{\varphi_1=30°, \phi=62°, \varphi_2=30°\}$ was developed during the friction stir welding.

Key words: friction stir welding; titanium alloy; texture; orientation imaging microscopy

1 Introduction

Friction stir welding (FSW) has been used to weld a wide variety of metals and alloys, including nearly all types of Al alloys, some Mg alloys and Cu alloys. In recent years, friction stir welding of high melting temperature materials such as steels and titanium alloys has become a research hotspot [1,2]. However, there has been limited information in the archival literature regarding the FSW of titanium alloys [3−12].

Texture in commercial purity titanium and titanium alloys has attracted significant interest over the years because of the extensive use of these materials in aerospace and other industries. However, very few studies regarding the texture evolution in titanium alloys resulting from FSW have been published. REYNOLDS et al [8] found a torsion texture in FSW welds of body-centered cubic (BCC) Timetal 21S alloy. MIRONOV et al [9,10] examined the crystallography of transformed β microstructure in friction stir welded Ti−6Al−4V alloy by adopting an indirect modeling approach involving β grain reconstruction as well as by direct crystallographic measurements in the surviving β phase. MIRONOV et al [11] and FONDA and KNIPLING [12] also revealed the dominant shear texture in pure Ti and near α-Ti friction stir welds, respectively.

The goal of this work is the elucidation of the texture resulting from FSW of Ti−6Al−4V alloy. Orientation imaging microscopy (OIM) provides both microstructural and crystallographic texture information that allows a coupled analysis of changes in texture and microstructure [13]. In the present study, texture in the friction stir weld of Ti−6Al−4V alloy is studied by OIM.

2 Experimental

The material used in the present study, Ti−6Al−4V, belongs to the duplex titanium alloy. That is to say, high temperature β phase can be retained due to the addition of β stable element V [14]. Commercial rolling sheet with a thickness of 2 mm was used for all of the welding experiments. The as-received sheet was annealed to eliminate stress and stable microstructure. Welding specimens with sizes of 120 mm×50 mm were cut by electrical discharge machining (EDM) from the supplied sheet with the long direction perpendicular to the rolling direction. Welding specimens were then cleaned with

Foundation item: Project (2010CB731704) supported by the National Basic Research Program of China; Project (AWJ-M13-11) supported by State Key Laboratory of Advanced Welding and Joining, Harbin Institute of Technology, China; Project (2012M511470) supported by China Postdoctoral Science Foundation
Corresponding author: Li ZHOU; Tel: +86-631-5677156; E-mail: zhouli@hitwh.edu.cn
DOI: 10.1016/S1003-6326(14)63070-3

acetone to remove grease and coolant used during cutting. Acid pickling procedure was then conducted to remove surface oxides formed during EDM.

The FSW of specimens was performed with a special welding system designed by Harbin Institute of Technology, China. The pin tool was fabricated from a W−Re alloy rod with quite simple geometry, but the details are not given here for the intellectual property limitation. Welds were made along the longitudinal direction of the specimens (perpendicular to the rolling direction of the sheet) at a welding speed of 0.85 mm/s and at a tool rotation rate of 400 r/min. During the FSW, a 2.5° tilt was applied to the pin tool.

Microstructural evolution was examined by optical microscope (OM, Olympus-PMG3) and orientation imaging microscope (OIM, JEOL E733). The transverse weld cross-sections were cut by EDM and prepared by standard metallographic procedures. Samples were mounted in epoxy and ground with abrasive paper. OIM observation specimen was electrolytically polished in a solution of 900 mL CH_3COOH+60 mL $HClO_4$ at 248 K under an operation voltage of 30 V for 60 s. Specimen for OIM observation was performed in a JEOL E733 Superprobe with a HKL electron backscatter diffraction (EBSD) module. Specimens were observed at an electron accelerating voltage of 20 kV. The OIM data for the stir zone (SZ) were obtained at the mid-plane of the welding specimen on the weld centerline, while the OIM data for base material (BM) were obtained well away from the SZ. A step size of 0.5 μm was used and each datum set contained 40000 points. Texture was analyzed using the HKL CHANNEL 5 software.

3 Results and discussion

A typical OM macro-image of weld cross-section is revealed by etching with Kroll's reagent, as shown in Fig. 1. The thickness of the weld is nearly constant in the cross-section, indicating that there is little sheet thinning during the FSW. The central darker region corresponds to the refined microstructure in the SZ. The sideward lighter zone is the BM. The SZ seems like 'bowl-shape' and no volumetric defects were observed in the cross-section. In Fig. 1, RS and AS are the retreating and advancing sides of the welding tool, respectively. WD corresponds to the welding direction and is parallel to the TD. RD, ND and TD stand for rolling direction, normal direction and transverse direction of the sheet, respectively.

Fig. 1 OM macro image of typical weld cross-section

Figure 2 shows a higher magnification view of the boundary between BM and SZ on the AS by OIM. The BM has elongated primary *α* phase and transformed *β* due to the incomplete annealing after milling. The SZ is characterized by equiaxed primary *α* phase and transformed *β*. This indicates that the peak temperature during FSW was below the *β*-transus temperature [14].

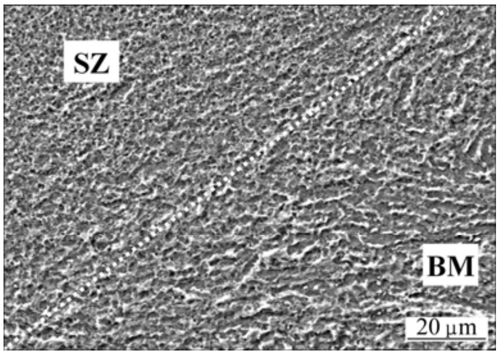

Fig. 2 Boundary between SZ and BM on AS by OIM

The grain morphology and the low-angle boundaries resulting from the dislocation structure are revealed by OIM, as shown in Fig. 3. The image is constructed such that misorientations greater than 15° between neighboring points have a thick boundary (black), and those from 2° to 15° have a thin boundary (red). The BM has elongated *α*+*β* with an average primary *α* grain size of 12 μm for grains defined by 15°

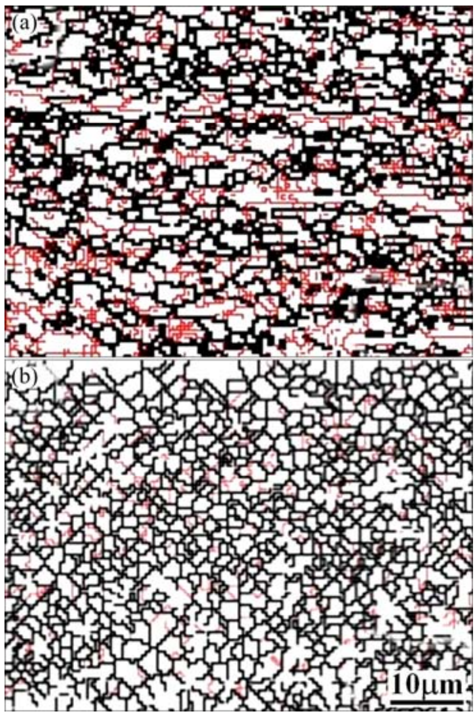

Fig. 3 Orientation images of region within BM (a) and SZ (b)

misorientation or greater based on the mean area method. The grain morphology in the SZ is equiaxed with primary α grain size reduced to about 7 μm due to the FSW. The grain boundary structure of the SZ varies only slightly in different positions within the equiaxed, recrystallized grain region.

It could be deduced from Fig. 3 that the grains in the mill annealed BM have recovered to some extent. The low-angle misorientations (red lines within the grains) observed within several of the grains could provide evidence of recovery during annealing [15]. However, the grains in the heavily deformed SZ mainly consist of high-angle boundaries. It could be deduced that dynamic recrystallization has occurred in the SZ due to significant plastic deformation and frictional heating during the FSW.

Figure 4 shows the misorientation angle histograms of the regions in the BM and the SZ. The BM has a high fraction of low-angle boundaries due to recovery in the annealing process. The overall distribution in the SZ differs remarkably from that in the BM, which has a higher fraction of high-angle boundaries due to the dynamically recrystallized structure. This result is coincident with the OIM images.

Texture studies have been focused on the face centered cubic (FCC) metals during cold and (or) hot working processes. As for FSW of Al alloy, the SZ experiences dynamic recrystallization and a predominant shear texture is developed in the weld assuming proper choice of reference frame. As for FSW of titanium alloy, the peak temperature can exceed the β-transus temperature and thus texture evolution may involve complicated solid-state transformation, especially for duplex titanium alloys [3,5]. However, the temperature in the SZ is below β-transus temperature under given welding conditions and the SZ mainly experiences dynamic recrystallization in the present study.

The Ti−6Al−4V sheets used have α phase taking approximately 90% in the phase composition, therefore the study of texture evolution is focused on α phase. Pole figures and orientation density function (ODF) were used to determine crystallographic texture in the BM and the SZ. All pole figures in the present study have been rotated about 90° along the rolling direction (perpendicular to the welding direction in the plane of the sheet) so that the welding direction corresponds to the vertical direction (TD) in the pole figures.

The texture in sheet hexagonal metals, is commonly represented by $\{h\ k\ i\ l\}\langle u\ v\ t\ w\rangle$, which means that the $\{h\ k\ i\ l\}$ planes of these grains lie parallel to the sheet plane, whereas their $\langle u\ v\ t\ w\rangle$ direction points parallel the rolling direction. The α phase {0002} and $\{01\bar{1}0\}$ pole figures in the BM are presented in Fig. 5. It indicates that

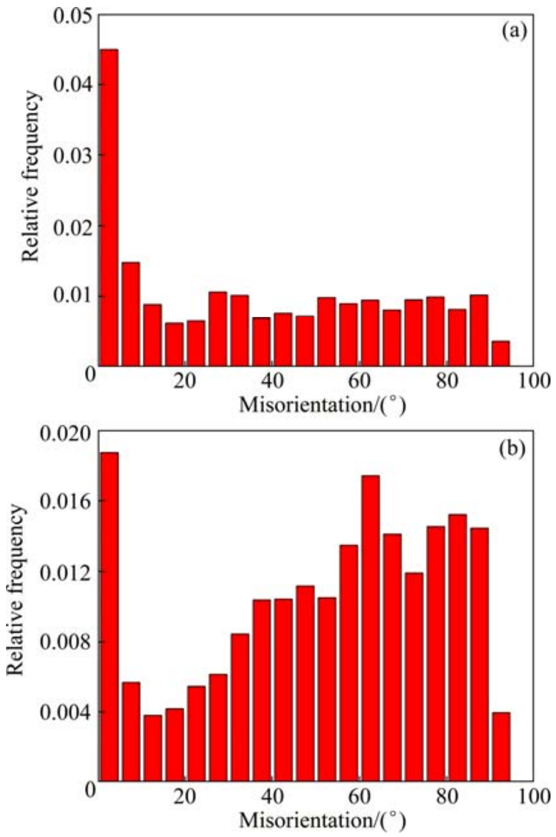

Fig. 4 Misorientation angle histograms for large region within BM (a) and SZ (b)

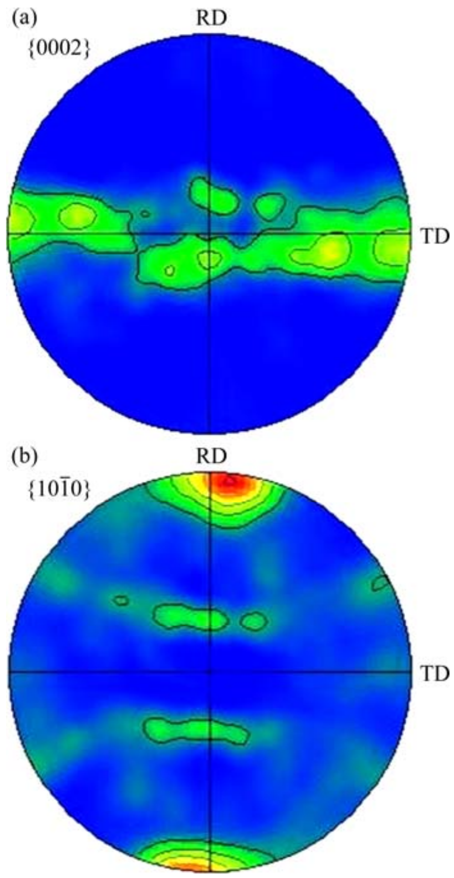

Fig. 5 {0002} (a) and $\{01\bar{1}0\}$ (b) pole figures of α phase in BM

the BM is characterized by a rolled texture, where the $\langle 10\bar{1}0\rangle$ poles aligned with the rolling direction and the $\langle 11\bar{2}0\rangle$ directions pointed parallel to the TD. From a deformation mechanism point of view, hexagonal close packed (HCP) metals are quite different from cubic metals in which limited slip systems are available and twinning frequently provides significant, but not dominant, deformation modes (Fig. 6). The texture of rolled hexagonal metals and alloys can be categorized into three groups according to their ratios of c/a. In general, the c/a ratio reflects the activation of the different slip systems. The HCP α phase possesses a c/a ratio of 1.587, which is less than the ideal c/a ratio of 1.633; slipping on prismatic planes is largely responsible for textures of these types with basal pole spreading [16]. This is the reason why the above textures with basal poles tilted away from the ND toward the TD are formed (see Fig. 5).

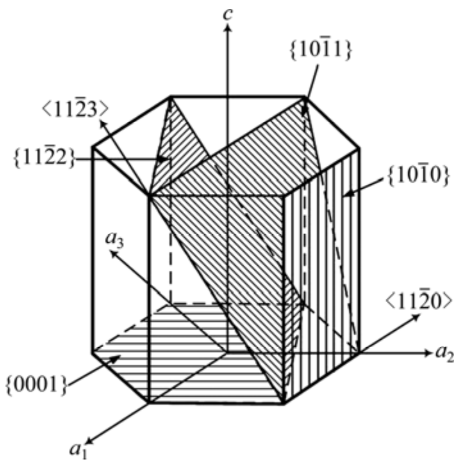

Fig. 6 Slip system in HCP metals

ODF sections at constant φ_2 of the SZ are presented in Fig. 7 and the Bunge system is adopted to define the Euler angles (see Fig. 8). In addition to the crystal symmetry in hexagonal materials, the Euler space was restricted to the region {π/2, π/2, π/3} [17]. It could be deduced from Fig. 7 that the main peak is centered at $\{\varphi_1=30°,\ \phi=62°,\ \varphi_2=30°\}$. A recrystallization texture characterized by a high density of the ODF around $\{\varphi_1=30°,\ \phi=62°,\ \varphi_2=30°\}$ was developed in low alloyed titanium sheets [18]. The texture components can be expressed as $(10\bar{1}3)[\bar{1}2\bar{1}0]$ according to the relationship between the orientation $g\{\varphi_1\ \phi\ \varphi_2\}$ and $\{h\ k\ i\ l\}\langle u\ v\ t\ w\rangle$ in the Bunge system. The texture in the SZ can be shown to correspond almost exactly to the recrystallization texture reported in Ref. [15] by rotation (−30°, −30°, 0°). It could be argued that the texture formed in the SZ was due to dynamic recrystallization. However, the texture components were rotated from the conventional recrystallization texture caused by grain rotation regarding the effect of the rotational FSW tool. The SZ grain rotation caused by the FSW tool was also reported by REYNOLDS et al [8].

4 Conclusions

1) Sound weld was produced in Ti−6Al−4V alloy sheet using a W−Re pin tool installed on a special welding system under proper welding parameters.

2) The BM was characterized by elongated primary α+transformed β with a rolled texture. The SZ was composed of equiaxed grains due to dynamic recrystallization and a texture around $\{\varphi_1=30°,\ \phi=62°,\ \varphi_2=30°\}$ was developed.

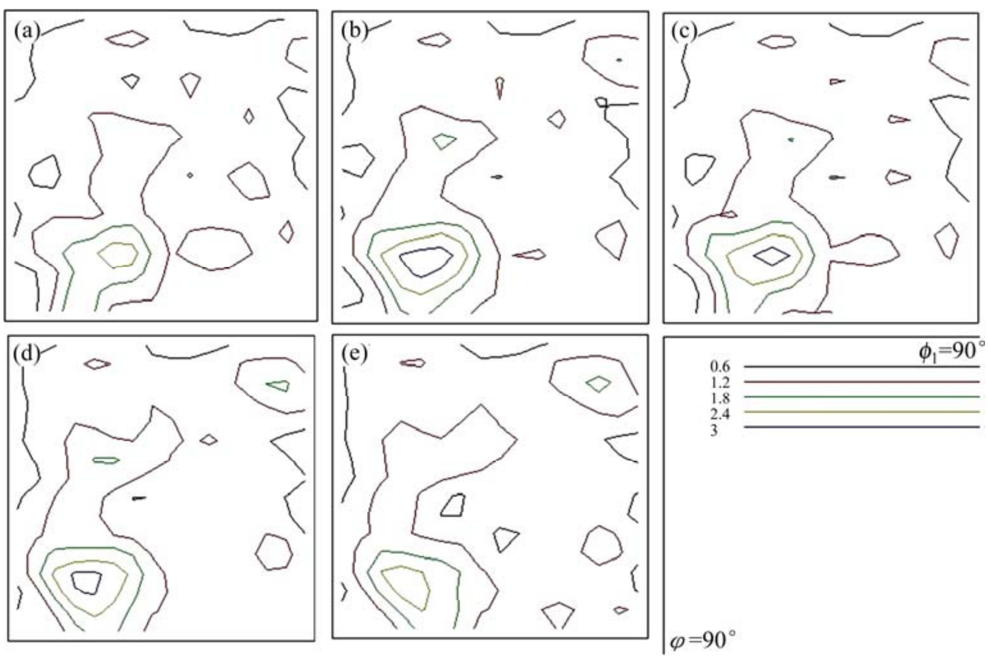

Fig. 7 ODF sections at constant φ_2 of SZ: (a) φ_2=30°; (b) φ_2=37°; (c) φ_2=33°; (d) φ_2=40°; (e) φ_2=43°

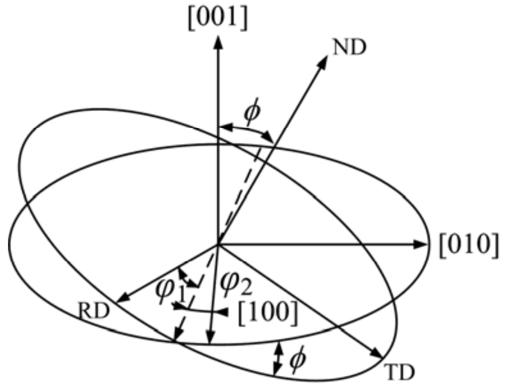

Fig. 8 Illustration of Euler angles in accordance with Bunge system

3) The SZ texture could be rotated in order to correspond to a recrystallization texture in Ti alloys. The required rotation was (−30°, −30°, 0°) in Euler space.

References

[1] MISHRA R S, MA Z Y. Friction stir welding and processing [J]. Materials Science and Engineering R, 2005, 50: 1−78.

[2] NANDAN R, DEBROY T, BHADESHIA H. Recent advances in friction-stir welding—Process, weldment structure and properties [J]. Progress in Materials Science, 2008, 53: 980−1023.

[3] RAMIREZ A J, JUHAS M C. Microstructural evolution in Ti−6Al−4V friction stir welds [J]. Materials Science Forum, 2003, 426: 2999−3004.

[4] LEE W B, LEE C Y, CHANG W S, YEON Y M, JUNG S B. Microstructural investigation of friction stir welded pure titanium [J]. Materials Letters, 2005, 59: 3315−3318.

[5] ZHANG Y, SATO Y S, KOKAWA H, PARK S H C, HIRANO S. Microstructural characteristics and mechanical properties of Ti−6Al−4V friction stir welds [J]. Materials Science and Engineering A, 2008, 485: 448−455.

[6] ZHANG Y, SATO Y S, KOKAWA H, PARK S H C, HIRANO S. Stir zone microstructure of commercial purity titanium friction stir welded using PCBN tool [J]. Materials Science and Engineering A, 2008, 488: 25−30.

[7] LIU H J, ZHOU L. Microstructural zones and tensile characteristics of friction stir welded joint of TC4 titanium alloy [J]. Transactions of Nonferrous Metals Society of China, 2010, 20(10): 1873−1878.

[8] REYNOLDS A P, HOOD E, TANG W. Texture in friction stir welds of Timetal 21S [J]. Scripta Materialia, 2005, 52: 491−494.

[9] MIRONOV S, ZHANG Y, SATO Y S, KOKAWA H. Development of grain structure in beta-phase field during friction stir welding of Ti−6Al−4V alloy [J]. Scripta Materialia, 2008, 59: 27−30.

[10] MIRONOV S, ZHANG Y, SATO Y S, KOKAWA H. Crystallography of transformed beta microstructure in friction stir welded Ti−6Al−4V alloy [J]. Scripta Materialia, 2008, 59: 511−514.

[11] MIRONOV S, SATO Y S, KOKAWA H. Development of grain structure during friction stir welding of pure titanium [J]. Acta Materialia, 2009, 57: 4519−4528.

[12] FONDA R W, KNIPLING K E. Texture development in near α-Ti friction stir welds [J]. Acta Materialia, 2010, 58: 6452−6463.

[13] BUNGE H J, SCHWARZER R A. Orientation stereology—A new branch in texture research [J]. Advanced Engineering Materials, 2001, 3: 25−39.

[14] POLMEAR I J. Light alloys metallurgy of the light metals [M]. 3rd ed. London: Edward Arnold, 1995.

[15] HUMPHREYS F J, HATHERLY M. Recrystallization and related annealing phenomena [M]. 2nd ed. Amsterdam: Elsevier, 2004.

[16] REED-HILL R E, ABBASCHIAN R. Physical metallurgy principles [M]. 3rd ed. Boston: PWS-KENT Publishing Co, 1992.

[17] RANDLE V, ENGLER O. Introduction to texture analysis-macrotexture, microtexture and orientation mapping [M]. New York: Gordon and Breach Science Publishers, 2000.

[18] WAGNER F, BOZZOLO N, van LANDUYT O, GROSDIDIER T. Evolution of recrystallisation texture and microstructure in low alloyed titanium sheets [J]. Acta Materialia, 2002, 50: 1245−1259.

Ti−6Al−4V 钛合金搅拌摩擦焊缝的织构

周 利[1,2,3]，刘会杰[1]，吴林志[3]

1. 哈尔滨工业大学 先进焊接与连接国家重点实验室，哈尔滨 150001；
2. 哈尔滨工业大学(威海) 山东省特种焊接技术重点实验室，威海 264209；
3. 哈尔滨工业大学 复合材料与结构研究所，哈尔滨 150001

摘 要：采用 W−Re 合金搅拌头对 $\alpha+\beta$ 双相 Ti−6Al−4V 钛合金进行搅拌摩擦焊并在合适的工艺参数下获得无缺陷焊缝，利用取向成像显微镜对 Ti−6Al−4V 钛合金搅拌摩擦焊缝的织构进行研究。Ti−6Al−4V 钛合金母材为轧制退火态，组织由变形的初生 α 相和转变 β 组织构成，具有典型的轧制织构。焊核区组织与母材明显不同，由大量的等轴动态再结晶晶粒组成，并在搅拌摩擦焊过程中形成{φ_1=30°，ϕ=62°，φ_2=30°}取向的织构。

关键词：搅拌摩擦焊；钛合金；织构；取向成像显微镜

(Edited by Xiang-qun LI)